

Co-ordination chemistry of 3*S*-aminopyrrolidine and 3*S*-(methylamino)pyrrolidine: crystallisation of the two diastereomers of dichloro[3*S*-(*R,S*-methylamino)pyrrolidine]palladium(II)

Paul D. Newman,* Michael B. Hursthouse and K. M. Abdul Malik

Department of Chemistry, Cardiff University, PO Box 912, Park Place, Cardiff, UK CF1 3TB. E-mail: newmanp1@cardiff.ac.uk

Received 17th November 1998, Accepted 22nd December 1998

Complexes of divalent Cu, Ni, Pd and Pt with 3*S*-aminopyrrolidine (*S*-ap) have been prepared and characterised by a combination of NMR, CD, electronic, IR and microanalytical techniques. The chosen chirality of the stereogenic carbon (*S*) forces the secondary nitrogen to adopt the *R* stereochemistry on co-ordination with the conformation of the 5-membered chelate being λ . The planar $[M(S\text{-ap})_2]^{2+}$ complexes exist as a mixture of *cis* and *trans* isomers in the solid state and in solution. The *trans* arrangement is forced upon co-ordination of an axial donor (X = halide, thiocyanate or nitrite) in the five-co-ordinate ions $[Cu(S\text{-ap})_2X]^+$. Methylation of the primary amine of *S*-ap generates another secondary nitrogen centre in the new ligand 3*S*-(methylamino)pyrrolidine, *S*-meap. This exocyclic nitrogen is not restricted to a single configuration on co-ordination. The complexes $[M(S\text{-meap})Cl_2]$, where M = Pd or Pt, have been prepared and characterised. Both diastereoisomers (*R*- and *S*-N_{Me}) of $[Pd(S\text{-meap})Cl_2]$ crystallise from aqueous solution as distinct crystal forms which can be separated by mechanical means. The structure of the N_{Me}(*R*) isomer has been determined by X-ray crystallography.

Introduction

The diamines represent one of the most extensively studied classes of bidentate ligands, to the point that the archetypal member, 1,2-diaminoethane (*en*), has been referred to as ‘‘God’s gift to the co-ordination chemist’’.¹ Much of the fascination with these ligands has been concerned with the formation of optical isomers, where the source of chirality may be configurational, conformational, vicinal, or a combination of two or more of these elements. Recent interest has stemmed from their potential use as anticancer agents of the cisplatin $[Pt(NH_3)_2Cl_2]$ type with the premise that optically active amines may be more efficient in the chiral media of living organisms.

3*S*-Aminopyrrolidine (*S*-ap) is a commercially available chiral diamine that has been little studied as a donor to metal ions, although several platinum(II) complexes of the parent ligand and substituted derivatives have been investigated in anti-tumour treatments.^{2,3} Aspects of its co-ordination chemistry are discussed in the present paper. In addition, the novel methylated derivative 3(*S*)-(methylamino)pyrrolidine, *S*-meap, has been prepared and complexes with Pd^{II} and Pt^{II} synthesized and characterised. Both possible isomers of $[Pd(S\text{-meap})Cl_2]$, where the chirality at N_{Me} is *R* or *S*, have been isolated by mechanical separation of their distinct crystal forms. Each pure isomer rapidly inverts on dissolution to give an equilibrium mixture of the two diastereoisomers. The ready isolation of both asymmetric forms of a co-ordinated non-heterocyclic nitrogen is unusual for Pd^{II}, contrasting with the easy access to similar chiral species in platinum(II) systems.⁴

Results and discussion

Complexes of 3*S*-aminopyrrolidine (*S*-ap)

The compound *S*-ap is a stereochemically rigid diamine that co-ordinates to a metal centre to form a five-membered chelate with λ conformation and a larger fused six-membered chelate with an asymmetric boat geometry. The chiral carbon centre (*S*) forces the heterocyclic nitrogen to assume the *R* configura-

tion on co-ordination. The presence of two distinct N-donors in *S*-ap may give *cis* or *trans* isomers in square planar $M(L)_2$ complexes: one or other may be preferred on kinetic and/or thermodynamic grounds.

The CD spectrum of $[Cu(S\text{-ap})_2]^{2+}$ in aqueous solution has a $-,+$ pattern from high wavelength in the visible region, as observed for the related 3*S*-aminohexahydroazepine (*S*-ahaz) complex.⁵ The $\Delta\epsilon_{\max}$ value for the *S*-ap–Cu^{II} complex is, however, a factor of 10 lower than that of the *S*-ahaz species, even though both have equivalent chiral carbons (*S*), nitrogens (*R*) and chelate conformations (λ). Comparison of the more pertinent *g* factors ($\Delta\epsilon/\epsilon$) is not possible as the previous workers did not include isotropic spectral details with the CD results.⁵ The low $\Delta\epsilon_{\max}$ values for the copper(II) complex of *S*-ap relative to its larger ring analogue may be a reflection of different proportions of *cis* and *trans* isomers at equilibrium in the two systems. For the $[Ni(S\text{-ap})_2][ClO_4]_2$ complex single linear and CD positive maxima are observed. These single symmetrical bands are typical of square-planar nickel(II).

The electronic spectra of $[Pd(S\text{-ap})Cl_2]$ and $[Pd(S\text{-ap})_2]^{2+}$ consist of single maxima at $\lambda = 372$ and 289 nm, respectively. The two spin and magnetic-dipole allowed d–d transitions expected for Pd^{II} are resolved in the CD spectra (Figs. 1 and 2). The lower energy maxima of negative sign are assigned to the $^1A_1 \rightarrow ^1A_2$ transition and the higher energy, positive CD bands to the $^1A_1 \rightarrow ^1E$ transition. The small negative maximum at 356 nm in the CD of $[Pd(S\text{-ap})Cl_2]$ may arise from: (i) a spin-forbidden absorption of 3A_2 or 3E origin; (ii) the magnetic-dipole forbidden (spin-allowed) 1B_1 transition; or (iii) removal of the 1E degeneracy. None of these possibilities is discounted, although (i) is least likely as it is generally accepted that in systems such as these both spin-forbidden bands occur to low energy of the 1A_2 band. The CD spectrum of $[Pd(S\text{-ap})_2]^{2+}$ consists of two bands at 321 ($\Delta\epsilon = -2.87$) and 278 nm ($\Delta\epsilon = +6.84$ dm² mol⁻¹).

The electronic spectrum of $[Pt(S\text{-ap})(H_2O)_2]^{2+}$ contains two obvious maxima at 322 and 259 nm. The low molar absorption ($\epsilon = 530$ dm² mol⁻¹) of the low energy absorption suggests a

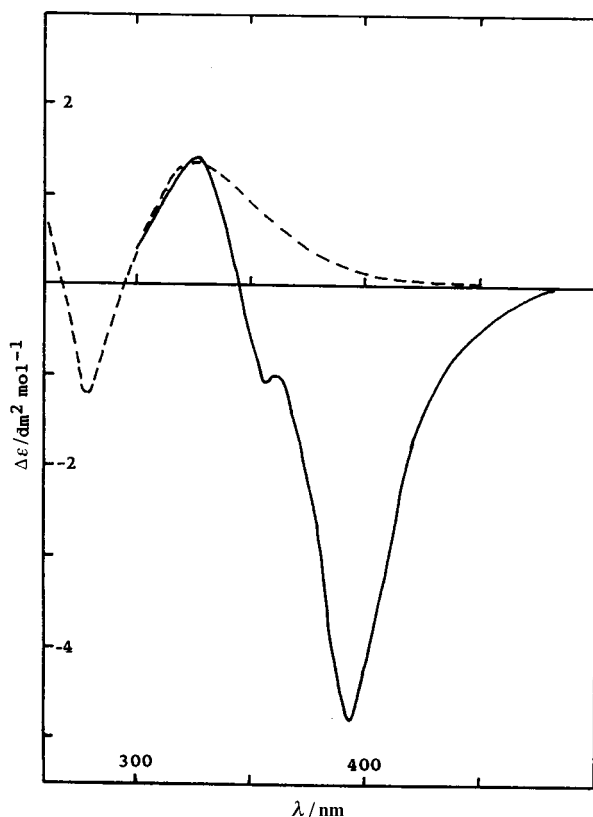


Fig. 1 The CD spectra of $[\text{Pd}(\text{S-ap})\text{Cl}_2]$ (—) and $[\text{Pt}(\text{S-ap})(\text{H}_2\text{O})_2]^{2+}$ (---) recorded in 0.2 M KCl and 1 M HClO_4 respectively.

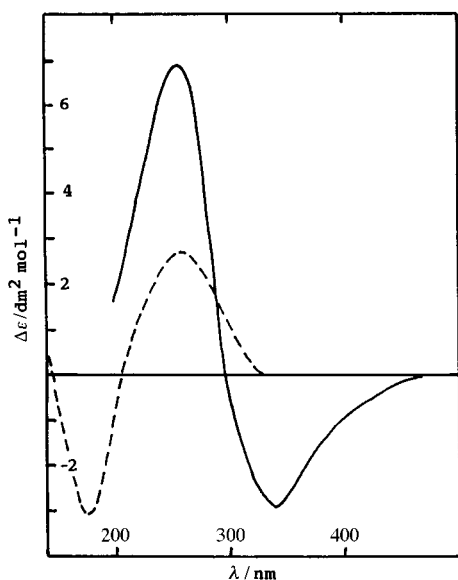


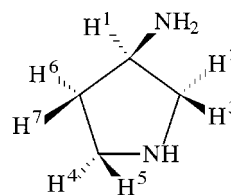
Fig. 2 The CD spectra of $[\text{Pd}(\text{S-ap})_2][\text{PF}_6]_2$ (—) and $[\text{Pt}(\text{S-ap})_2]\text{ClO}_4[\text{PF}_6]$ (---) recorded in aqueous solution.

spin-forbidden transition of ${}^1\text{A}_1 \rightarrow {}^3\text{A}_2$ or ${}^3\text{E}$ origin. The higher energy absorption ($\epsilon = 2090 \text{ dm}^2 \text{ mol}^{-1}$) may be assigned to one or both of the spin and magnetic-dipole allowed d-d transitions (${}^1\text{A}_2$, ${}^1\text{E}$). Each of the isotropic bands are complemented by CD maxima at 324 ($\Delta\epsilon = +1.33$) and 277 nm ($\Delta\epsilon = -1.19 \text{ dm}^2 \text{ mol}^{-1}$) (Fig. 1). The same spectral patterns occur for $[\text{Pt}(\text{S-ap})(\text{NH}_3)_2]^{2+}$ and $[\text{Pt}(\text{S-ap})_2]^{2+}$ (see Experimental section). Inspection of the CD manifolds in Figs 1 and 2 would appear to suggest a reversal of Cotton effects on altering the metal from platinum to palladium. This is clearly not the case. The disparity is accounted for on the basis of the assignments for the various CD bands. As stated earlier, the long-wavelength positive CD maxima in the spectra of the platinum

complexes result from a spin-forbidden transition. The higher energy bands (negative $\Delta\epsilon_{\text{max}}$) may be assigned to the ${}^1\text{A}_2$ or ${}^1\text{E}$ transition. For Pd^{II} , both strong CD absorptions are, in accord with related systems,⁶⁻¹⁰ assigned to spin-allowed transitions: the long wavelength negative maxima arise from the ${}^1\text{A}_1 \rightarrow {}^1\text{A}_2$ absorption and the positive bands from the ${}^1\text{A}_1 \rightarrow {}^1\text{E}$ transition. The CD signs associated with the palladium complexes are expected to be duplicated in the corresponding platinum analogues as established previously for a number of similar systems.⁶⁻¹¹ Hence, the negative bands in the CD spectra of the platinum(II) complexes are assigned to the ${}^1\text{A}_1 \rightarrow {}^1\text{A}_2$ transition; presumably the ${}^1\text{E}$ component lies out of range at $> 40000 \text{ cm}^{-1}$ [the CD curve does rise sharply around 260 nm for the mono(S-ap)platinum system suggesting a positive ${}^1\text{E}$ band].

For the mono(S-ap) complexes there are three sources of chirality that contribute to the observed CD spectra: the stereogenic carbon (S), the co-ordinated heterocyclic nitrogen (R) and the conformation of the 5-membered chelate ring (λ). Although not negligible, the vicinal effect of the stereogenic carbon is usually small and, in instances where it and a conformational chirality are all that contribute to any observed circular dichroism, the latter tends to dominate. Platinum(II) complexes of 1R,2R-diaminocyclohexane (R,R-chxn) have a λ conformation which gives positive CD signs for the ${}^1\text{A}_1 \rightarrow {}^1\text{E}$ transition whereas the ${}^1\text{A}_2$ band is largely unassigned.⁶ The complex $[\text{Pt}(\text{S-ap})(\text{H}_2\text{O})_2]^{2+}$ has a λ chelate and a negative $\Delta\epsilon_{\text{max}}$ for the ${}^1\text{A}_2$ absorption. It has been established that, in systems such as these, the asymmetric nitrogen tends to dominate the appearance of the CD spectrum.⁷⁻¹⁰ For means of comparison 2(S)-amino-1-(methylamino)propane (N-Me-S-pn) may be considered a linear analogue of S-ap: the former can be thought of as S-ap with the CH_2CH_2 bridge cleaved to generate the two methyl groups. Bosnich and Sullivan⁸ have resolved both diastereoisomers of $[\text{Pt}(\text{N-Me-S-pn})\text{Cl}_2]$ and shown the chiral nitrogen to be the controlling influence on the observed CD. The spectra of the S-ap complexes of Pd^{II} and Pt^{II} are very similar to the spectrum of N(R)- $[\text{Pt}(\text{N-Me-S-pn})\text{Cl}_2]$. Further, the CD manifold for $[\text{Pt}(\text{S-ap})(\text{NH}_3)_2]^{2+}$ is remarkably similar to that derived for the N(R) asymmetric nitrogen contribution in $[\text{Pt}(\text{meen})(\text{NH}_3)_2]^{2+}$ (meen = N-methyl-1,2-diaminoethane).

The ${}^1\text{H}$ NMR data for the palladium(II) and platinum(II) complexes are presented in Table 1 and Fig. 3; those for the $\text{Pt}(\text{S-ap})\text{Cl}_2$ complex accord with previous data.² Full analysis of the ${}^1\text{H}$ NMR of $[\text{Pt}(\text{S-ap})(\text{NH}_3)_2]\text{Cl}_2$ was achieved using homonuclear decoupling techniques. The ${}^1\text{H}$ spectrum is shown in Fig. 3 with assignments relative to the labelling scheme in I. The unique methine proton of the ring (H1), which neighbours four vicinal hydrogens, shows only one significant coupling ($J_{\text{H1-H2}} = 5.5 \text{ Hz}$). Consequently, the resonances of H2 and H3 occur as doublets ($J_{\text{gem}} = 10 \text{ Hz}$); ${}^{195}\text{Pt}$ - ${}^1\text{H}$ coupling is observed for H1, H2, H4 and H5 (Table 1). It has been shown that the ${}^3J_{\text{Pt-NCH}}$ coupling constants follow a Karplus-like dependence on dihedral angle;¹² the largest values of $J_{\text{Pt-H}}$ for $[\text{Pt}(\text{S-ap})(\text{NH}_3)_2]^{2+}$ are observed when the dihedral angle approaches 180° , e.g. $J_{\text{Pt-H2/H4}}$. The absolute value of ${}^3J_{\text{Pt-H3}}$ could not be determined, but is greater than zero as demonstrated by the 'bell-like' base of the resonance assigned to the proton concerned.



I

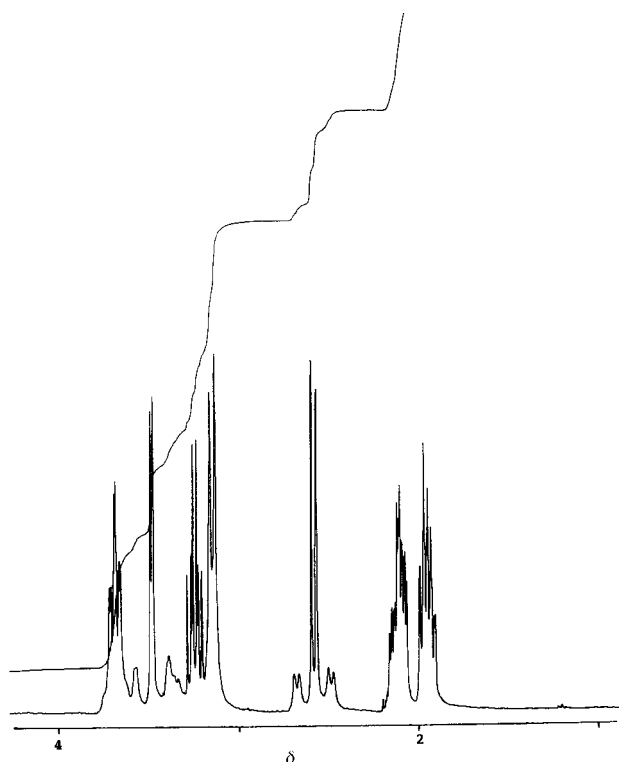


Fig. 3 The ^1H NMR spectrum of $[\text{Pt}(\text{S-ap})(\text{NH}_3)_2]\text{Cl}_2$ in D_2O .

It is evident from the NMR spectra of the $[\text{M}(\text{S-ap})_2]^{2+}$ complexes ($\text{M} = \text{Pd}$ or Pt) that both *cis* and *trans* forms are present in solution. In the case of the more labile palladium(II) species the ratio of isomers is probably a consequence of thermodynamic factors, contrasting with the platinum(II) analogue where this ratio is controlled by kinetic influences. The *cis/trans* ratios estimated by integration are 1.4 and 1.2:1 for the complexes of Pd^{II} and Pt^{II} respectively; both form the same isomer preferentially, although it was not easy to determine which one this was. All the signals of the predominant isomer, except that for H1, are shifted to low field relative to the less abundant species (this is also true of the C–H1 carbon in the ^{13}C NMR spectra). Computer-assisted molecular modelling has shown the ‘internal’ hydrogens (those projecting toward the metal) to be more crowded in the *trans* amine isomer, resulting in these protons being less shielded than in the *cis* form. This would suggest, though it does not prove, that the *trans* form is dominant for Pd^{II} and for Pt^{II} .

Five-co-ordinate complexes of *S-ap*

The ready propensity of Cu^{II} to co-ordinate an axial ligand(s) allowed the isolation of a number of heteroanion compounds where one of the counter ions was bound at a fifth site to give complexes of the type $[\text{Cu}(\text{S-ap})_2\text{X}]\text{ClO}_4$, where $\text{X} = \text{Cl}^-$, Br^- , I^- , NO_2^- or SCN^- . Conductance measurements show the compounds to be dissociated in water giving the aquated $[\text{Cu}(\text{S-ap})_2]^{2+}$ species. The axially bound monodentate (pseudo)-halide is retained on dissolution in nitromethane where conductivity values typical of 1:1 electrolytes were observed. The structure of the ternary cations is believed to be a square-based pyramid with *trans* nitrogens, as for the analogous complexes of *S-ahaz* and 3*S-aminopiperidine* (*S-apip*).¹³

Electronic and CD spectral results for the complexes are given in the Experimental section, with typical spectra shown in Fig. 4. The electronic spectra in solution consist of a single, broad, largely uninformative composite absorption band. Previously, square pyramidal copper(II) complexes have been said to give two characteristic absorption bands in the visible and near infrared region.^{13,14} For the present series of complexes

Table 1 ^1H NMR details for the complexes of *S-ap*^a

Complex	Assignment ^b	δ	J/Hz
<i>S-ap</i> ·2HCl	H1	3.84 (m)	
	H2, H3	3.50 (obs)	
	H4, H5	3.62 (m), 4.19 (m)	
	H6, H7	2.59 (m), 2.23 (m)	
$[\text{Pd}(\text{S-ap})(\text{H}_2\text{O})_2]^{2+}$	H1	3.27 (s)	
	H2, H3	2.20 (obs), 3.21 (d)	
	H4, H5	2.70 (m), 3.83 (br)	
	H6, H7	2.20 (obs)	
$[\text{Pt}(\text{S-ap})(\text{H}_2\text{O})_2]^{2+}$	H1	3.14 (obs)	
	H2, H3	2.34 (d)	
	H4, H5	3.14 (obs), 3.75 (m)	
	H6, H7	2.05 (obs)	
$[\text{Pt}(\text{S-ap})(\text{NH}_3)_2]\text{Cl}_2$	H1	3.47 (d)	$J_{\text{H1-H2}}$ 5.5
	H2, H3	2.58 (d), 3.14 (d)	$J_{\text{H1-H3}}$ 1.0
	H4, H5	3.23 (m), 3.68 (m)	$J_{\text{H2-H3}}$ 10.0
	H6, H7	2.11 (m), 1.96 (m)	$J_{\text{H2-H6}}$ 1.5
			$J_{\text{H3-H5}}$ 1.5
			$J_{\text{H4-H5}}$ 10.0
		$J_{\text{H4-H6}}$ 10.0	
		$J_{\text{H4-H7}}$ 7.0	
		$J_{\text{H5-H7}}$ 10.0	
		$J_{\text{H6-H7}}$ 10.5	
		$J_{\text{Pt-H1}}$ 64	
		$J_{\text{Pt-H2}}$ 70	
		$J_{\text{Pt-H4}}$ 70	
		$J_{\text{Pt-H5}}$ 32	
$[\text{Pd}(\text{S-ap})_2]\text{F}_2$	H1	3.57 (d), ^c 3.50 (d)	
	H2, H3	2.48 (dd), 2.43 (dd)	
	H4, H5	3.09 (d), 3.06 (d)	
	H6, H7	2.95 (m), 2.88 (m)	
		3.73 (m), 3.64 (m)	
		2.16 (m), 1.92 (m)	
$[\text{Pt}(\text{S-ap})_2]\text{ClO}_4\text{F}$	H1	3.48 (d), 3.39 (d)	
	H2, H3	2.57 (dd), 2.49 (dd)	
	H4, H5	3.06 (d), 3.01 (d)	
	H6, H7	3.29 (m), 3.21 (m)	
		3.72 (m), 3.65 (m)	
		2.07 (m), 1.87 (m)	

^a Spectra recorded in D_2O . ^b With respect to the labelling scheme shown. ^c Data in italics refer to the minor isomer of the bis(ligand) complexes.

these two bands are not distinct in the electronic spectra but are more readily distinguished in the CD (see below). The position of λ_{max} depends on the nature of the axial ligand, and shifts to longer wavelengths for $[\text{Cu}(\text{S-ahaz})_2\text{X}]^+$ as the position of X increases in the spectrochemical series.¹³ By contrast, the reverse dependence is observed for the analogous $[\text{Cu}(\text{S-apip})_2\text{X}]^+$ complexes;¹³ this is attributed to axial ligand dependent steric effects forcing the copper(II) ion to reside out of the N_4 plane. For the complexes of *S-ap*, λ_{max} shifts to higher wavelength along the series $\text{I}^- < \text{Br}^- < \text{Cl}^-$ for the halides, in accord with the *S-ahaz* system: the thiocyanate and nitrite species are to high energy of the halides in the present complexes. With respect to the analysis of Miyamura *et al.*,¹³ it would seem that little out-of-plane distortion occurs on co-ordination of an axial donor in $[\text{Cu}(\text{S-ap})_2\text{X}]^+$, where $\text{X} = \text{Cl}^-$, Br^- or I^- , but may occur to some degree in the SCN^- and NO_2^- systems. This behaviour is intermediate between that observed for the higher homologues *S-apip* and *S-ahaz*.¹³

The CD spectra of the five-co-ordinate species fall essentially into two groups, typified by the bromo and iodo complexes in Fig. 4. All have their most intense CD absorptions ($\Delta\epsilon$ values all positive) at long wavelength (centred at ≈ 750 nm and trailing into the near infrared), presumably associated with the $d_{xy} \rightarrow d_{x^2-y^2}$ electronic transition. The distinction between the two classes occurs at higher energy where the chloro and bromo

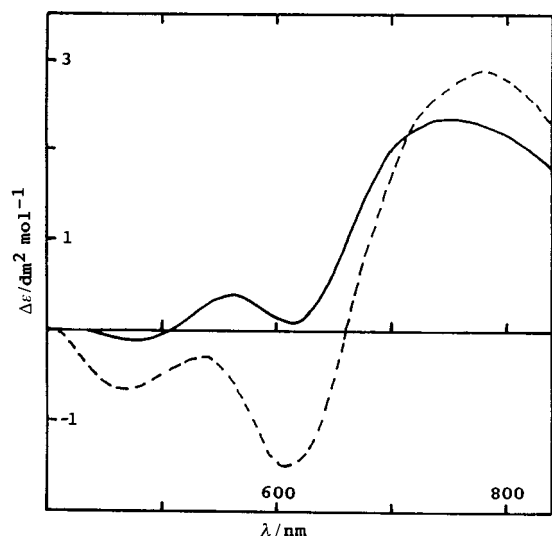


Fig. 4 The CD spectra of $[\text{Cu}(\text{S-ap})_2\text{Br}]\text{ClO}_4$ (—) and $[\text{Cu}(\text{S-ap})_2\text{I}]\text{ClO}_4$ (---) recorded in nitromethane solution.

species have single positive maxima of low intensity, as opposed to the two negative lobes observed for the iodo and thiocyanate complexes. The nitrite system is anomalous, possessing a $-,+$ pattern in the region of the second CD band. The reasons for these differences remain obscure, but it is likely that slight variations in structure, notably the disposition of Cu^{II} within the basal plane, and the possible presence of linkage isomers of NO_2^- are responsible for the disparate CD spectra.

Complexes of *S*-meap

Monomethylation of the primary amine of *S*-ap generates a second prochiral nitrogen that, unlike the heterocyclic nitrogen, may adopt either the *R* or *S* stereochemistry upon coordination. When complexed to a labile metal ion such as Cu^{2+} or Ni^{2+} both configurations would be expected to exist in facile equilibrium; the coexistence of *cis/trans* equilibria further complicates these systems. In Pd^{2+} and Pt^{2+} complexes the N_{Me} nitrogen may invert freely in solution *via* vibrational (umbrella) motion, or be restricted if the isomerisation requires the breaking of the $\text{M}-\text{N}_{\text{Me}}$ bond.

The synthesis of $[\text{Pd}(\text{S-meap})\text{Cl}_2]$ gave two distinct crystal forms from aqueous solution: thin yellow plates and blocky orange prisms. The structure of the more robust orange form as determined by single crystal X-ray analysis is shown in Fig. 5, and selected bond lengths and angles are given in Table 2. The geometry is, as expected, square planar, with the chlorides necessarily *cis*. The small bite of the diamine contracts the $\text{N}-\text{Pd}-\text{N}$ angle to $82.26(11)^\circ$, with a concomitant increase in the $\text{Cl}-\text{Pd}-\text{Cl}$ angle to $94.76(3)^\circ$. Distortions in the square planar geometry are also evident in the angles involving the *trans* ligands, $\text{Cl}(1)-\text{Pd}(1)-\text{N}(1)$ $173.50(8)^\circ$ and $\text{Cl}(2)-\text{Pd}(1)-\text{N}(2)$ $173.24(8)^\circ$, which are *ca.* 7° narrower than the ideal value 180° . The two $\text{Pd}-\text{Cl}$ [$2.3005(8)$ and $2.3204(9)$ Å] and two $\text{Pd}-\text{N}$ [$2.038(3)$ and $2.054(3)$ Å] bond lengths are slightly asymmetric, and these are comparable with those in other related complexes.^{15,16} The absolute configuration of the chiral carbon (*S*) and heterocyclic nitrogen (*R*) are as dictated by the original choice of chiral asparagine precursor. The stereochemistry at the non-ring nitrogen is *R* with the methyl group projecting out of the co-ordination plane with the $\text{N}(1)-\text{Pd}(1)-\text{N}(2)-\text{C}(5)$ torsion angle of $115.6(3)^\circ$. The five-membered chelate has a flattened λ conformation. Both the NH groups in the molecule are involved in intermolecular hydrogen bonding which is responsible for holding together the individual molecules in the crystal. The dimensions of these hydrogen bonds are: (i) $\text{N}(1)-\text{H}(1)\cdots\text{Cl}(1)$ ($-1+x, y, z$) $\text{N}(1)\cdots\text{Cl}(1)$ 3.281 , $\text{H}(1)\cdots\text{Cl}(1)$ 2.594 Å, $\text{N}(1)-\text{H}(1)-\text{Cl}(1)$ 133° ; (ii) $\text{N}(2)-\text{H}(2)\cdots\text{Cl}(2)$ ($1-x, x,$

Table 2 Bond lengths (Å) and angles ($^\circ$) for $\text{N}(\text{R})-[\text{Pd}(\text{S-meap})\text{Cl}_2]$

$\text{Pd}(1)-\text{N}(1)$	2.038(3)	$\text{Pd}(1)-\text{N}(2)$	2.054(3)
$\text{Pd}(1)-\text{Cl}(1)$	2.3005(8)	$\text{Pd}(1)-\text{Cl}(2)$	2.3204(9)
$\text{N}(1)-\text{C}(4)$	1.487(4)	$\text{N}(1)-\text{C}(1)$	1.498(5)
$\text{N}(2)-\text{C}(5)$	1.479(4)	$\text{N}(2)-\text{C}(3)$	1.489(5)
$\text{C}(1)-\text{C}(2)$	1.529(5)	$\text{C}(2)-\text{C}(3)$	1.525(5)
$\text{C}(3)-\text{C}(4)$	1.510(5)		
$\text{N}(1)-\text{Pd}(1)-\text{N}(2)$	82.26(11)	$\text{N}(1)-\text{Pd}(1)-\text{Cl}(1)$	173.50(8)
$\text{N}(2)-\text{Pd}(1)-\text{Cl}(1)$	91.29(9)	$\text{N}(1)-\text{Pd}(1)-\text{Cl}(2)$	91.64(8)
$\text{N}(2)-\text{Pd}(1)-\text{Cl}(2)$	173.24(8)	$\text{Cl}(1)-\text{Pd}(1)-\text{Cl}(2)$	94.76(3)
$\text{C}(4)-\text{N}(1)-\text{C}(1)$	102.6(3)	$\text{C}(4)-\text{N}(1)-\text{Pd}(1)$	105.6(2)
$\text{C}(1)-\text{N}(1)-\text{Pd}(1)$	107.4(2)	$\text{C}(5)-\text{N}(2)-\text{C}(3)$	113.9(3)
$\text{C}(5)-\text{N}(2)-\text{Pd}(1)$	113.9(2)	$\text{C}(3)-\text{N}(2)-\text{Pd}(1)$	104.8(2)
$\text{N}(1)-\text{C}(1)-\text{C}(2)$	102.2(3)	$\text{C}(3)-\text{C}(2)-\text{C}(1)$	105.0(3)
$\text{N}(2)-\text{C}(3)-\text{C}(4)$	106.1(3)	$\text{N}(2)-\text{C}(3)-\text{C}(2)$	110.0(3)
$\text{C}(4)-\text{C}(3)-\text{C}(2)$	103.0(3)	$\text{N}(1)-\text{C}(4)-\text{C}(3)$	97.7(3)

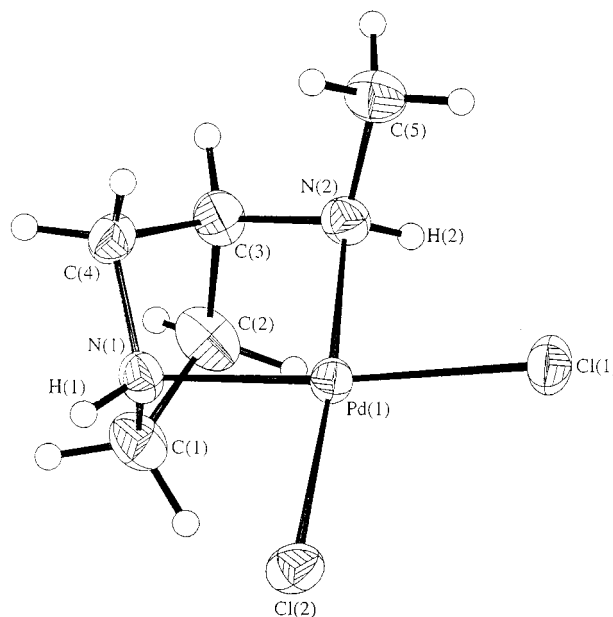


Fig. 5 Solid state structure of $\text{N}(\text{R})-[\text{Pd}(\text{S-meap})\text{Cl}_2]$ showing the atom labelling scheme used. The thermal ellipsoids are drawn at 40% probability level.

$0.5 + y, 0.5 - z$) $\text{N}(2)\cdots\text{Cl}(2)$ 3.373 , $\text{H}(2)\cdots\text{Cl}(2)$ 2.544 Å, $\text{N}(2)-\text{H}(2)-\text{Cl}(2)$ 152° . The influence of hydrogen bonding in cases of conglomerate crystallisation has been well established by Bernal.¹⁷ Unusually, in the present case where the N_{Me} centre rapidly inverts in aqueous solution it would appear that both forms, orange $\text{N}_{\text{Me}}(\text{R})$ and yellow $\text{N}_{\text{Me}}(\text{S})$, are crystallised concurrently from this medium. It is possible that the yellow plates are a second crystal form of the $\text{N}_{\text{Me}}(\text{R})$ isomer. However, the fact that the sum of the solid-state CD spectra for the two crystal forms gives, qualitatively, the solution spectrum coupled with the knowledge that both forms are present in solution (see below) leads to the likely conclusion that the thin yellow plates are the $\text{N}_{\text{Me}}(\text{S})$ diastereomer.†

Chiroptical results for the *S*-meap complexes are presented in Figs. 6 and 7. Compared to the homologous compounds of *S*-ap, those of *S*-meap show hypsochromic shifts in both the electronic and CD spectra. Thus, methylation of the non-ring nitrogen results in a decrease of the ligand field generated by the diamine. For Cu^{II} and Ni^{II} , the CD spectra of the bis(*S*-meap) and bis(*S*-ap) complexes are qualitatively analogous, although little comparison is possible here, as in these labile systems a number of competing isomeric equilibria are expected in solu-

† This is demonstrated by the NMR and circular dichroism measurements that follow.

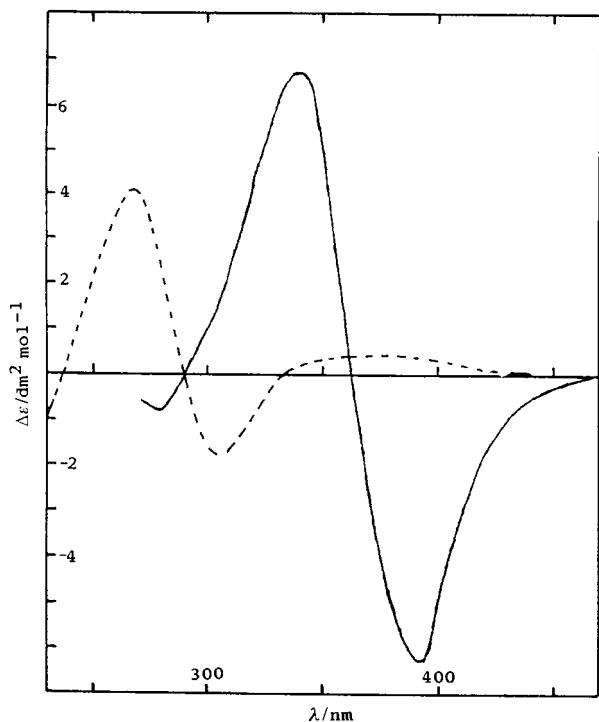


Fig. 6 The spectra of $[\text{Pd}(\text{S-meap})\text{Cl}_2]$ (—) and $[\text{Pt}(\text{S-meap})\text{Cl}_2]$ (---) recorded in 2 M HCl and 0.2 M KCl respectively.

tion (see above). The solution CD spectrum of $[\text{Pd}(\text{S-meap})\text{Cl}_2]^\ddagger$ resembles the curve for $[\text{Pd}(\text{S-ap})\text{Cl}_2]$, but it is noteworthy that the $\Delta\epsilon_{\text{max}}$ values are appreciably larger for the *N*-methyl derivative, especially for the ${}^1\text{A}_1 \rightarrow {}^1\text{E}$ transition. Three maxima are evident in both the isotropic and chiroptic spectra of $[\text{Pt}(\text{S-meap})\text{Cl}_2]$ (see Experimental section and Fig. 6). The low absorption coefficient ($\epsilon = 480 \text{ dm}^2 \text{ mol}^{-1}$) of the long wavelength isotropic band ($\lambda = 355 \text{ nm}$) characterises it as a singlet \rightarrow triplet transition. As observed in the (*S*-ap)-Pt systems the CD component associated with this spin-forbidden excitation has a positive $\Delta\epsilon_{\text{max}}$ ($+0.44 \text{ dm}^2 \text{ mol}^{-1}$ at 379 nm). Unlike the platinum *S*-ap complexes, both spin-allowed transitions are observed in the electronic and chiroptic spectra of $[\text{Pt}(\text{S-meap})\text{Cl}_2]$. The maximum at 303 nm in the electronic spectrum is assigned to the ${}^1\text{A}_2$ band which has a corresponding CD maximum at 305 nm with $\Delta\epsilon_{\text{max}} = -1.80 \text{ dm}^2 \text{ mol}^{-1}$: this is further support for the somewhat tentative assignment in the *S*-ap system. The ${}^1\text{A}_1 \rightarrow {}^1\text{E}$ transition that was not observed in the mono(*S*-ap)-platinum complexes§ occurs as a shoulder in the isotropic spectrum and a strongly positive maximum in the CD spectrum. The CD curves for the platinum and palladium analogues are comparable.

The solid-state CD spectra of $\text{N}(\text{R})\text{-}[\text{Pd}(\text{S-meap})\text{Cl}_2]$ and $\text{N}(\text{S})\text{-}[\text{Pd}(\text{S-meap})\text{Cl}_2]$ as KBr discs are shown in Fig. 7. The curves shown in Fig. 7 are the average of 3–6 independent spectra for each complex. The spectra of the $[\text{Pd}(\text{S-meap})\text{Cl}_2]$ complexes showed very little variation between samples, however the solid-state spectra of $[\text{Pd}(\text{S-ap})\text{Cl}_2]$ were highly variable and quite unlike its solution spectrum. Such disparity between solution and solid-state CD spectra is not easily explained, but may be the result of geometric constraints (and effects associated with differences in local symmetry) enforced by crystal packing in the solid that are not evident in solution. In addition, some halide exchange may have occurred to a varying

‡ It has been shown by NMR that the two diastereoisomers of $[\text{Pd}(\text{S-meap})\text{Cl}_2]$ equilibrate on dissolution to give equivalent spectra.

§ The ${}^1\text{E}$ component was lost to high energy in the comparable complexes of *S*-ap because of the stronger ligand field of H_2O and NH_3 relative to chloride, $[\text{Pt}(\text{S-ap})\text{Cl}_2]$ being too insoluble to allow electronic spectral analysis.

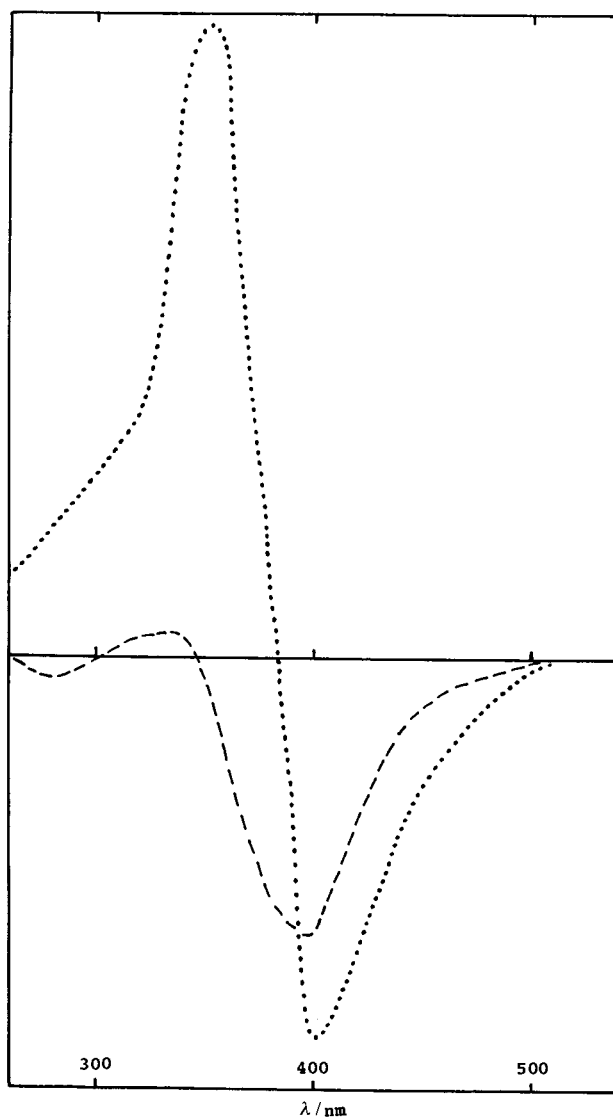


Fig. 7 Solid state CD spectra of $\text{N}(\text{R})\text{-}[\text{Pd}(\text{S-meap})\text{Cl}_2]$ (---) and $\text{N}(\text{S})\text{-}[\text{Pd}(\text{S-meap})\text{Cl}_2]$ (····) recorded as 1% suspensions in KBr.

degree between samples of $[\text{Pd}(\text{S-ap})\text{Cl}_2]$ in the solid state to produce the incongruous spectra. The sum of the spectra of the two crystalline forms of $[\text{Pd}(\text{S-meap})\text{Cl}_2]$ reproduce, in a qualitative way, the solution spectrum, supporting the assignment of the $\text{N}_{\text{Me}}(\text{S})$ stereochemistry in the yellow form. However, the solid-state spectra of the two forms, $\text{N}(\text{R})$ and $\text{N}(\text{S})$, do not exhibit an approximate enantiomorphism (Fig. 7): this situation is unlike that with the two isomers of $[\text{Pt}(\text{N}_{\text{Me}}\text{-S-pn})\text{Cl}_2]$.^{7,8} The absence of enantiomorphic behaviour for the $[\text{Pd}(\text{S-meap})\text{Cl}_2]$ system is explained on the basis of the inherent structural differences between the two possible isomers. The two diastereoisomers differ enough in structure that their CD spectra are not even approximately enantiomeric.

The ${}^1\text{H}$ NMR spectra of the $[\text{M}(\text{S-meap})(\text{D}_2\text{O})_2]^{2+}$ complexes, where $\text{M} = \text{Pd}$ or Pt , are complicated by overlapping multiplets between δ 1 and 4. The one distinct feature is the presence of two sharp singlets at δ 2.45 and 2.26 for the palladium(II) complex, and δ 2.55 and 2.37 for Pt^{II} . Each singlet is assigned to a single epimer (N_{Me} , *R* or *S*) of $[\text{M}(\text{S-meap})(\text{D}_2\text{O})_2]^{2+}$. This is clearer in the ${}^{13}\text{C}$ NMR spectra, where 10 peaks are observed, five for each isomer. The ratio of the two possible isomers is estimated by integration to be 61:39 and 57:43 for Pd^{2+} and Pt^{2+} respectively. It is not obvious from the NMR results which isomer is dominant, although it appears to be the same in both metal systems. The dissolution of pure

N(R)- or *N(S)*-[Pd(*S*-meap)Cl₂] in D₂O with or without added KCl gave essentially the same spectrum as observed for [Pd(*S*-meap)(D₂O)₂]²⁺, *i.e.* epimerisation occurs rapidly on dissolution, confirming the CD observations. The presence of distinct N_{Me} singlets for each diastereoisomer in the ¹H NMR of [Pd(*S*-meap)Cl₂] (separation 75 Hz) shows the epimerisation to be slow on the NMR timescale at ambient temperature. Inversion of the N_{Me} centre is considered to succeed Pd–N_{Me} bond rupture, as outlined for similar platinum(II) complexes.³ It was not possible to examine the relation between rates of epimerisation and N_{Me}-H exchange in organic solvents owing to the very low solubility of the complexes in such media. Compounds of the cations [M(*S*-meap)₂]²⁺ (M = Pd or Pt) were readily obtained, but not characterised, as initial NMR studies revealed a large degree of isomeric complexity for these systems.

Experimental

3-*S*-Aminopyrrolidine dihydrochloride (*S*-ap·2HCl) was obtained from Lancaster Synthesis Ltd., the free amine being extracted (diethyl ether) from a strongly basic solution prior to each synthesis. Removal of the organic solvent *in vacuo* gave the free base as a clear oil. All other reagents were of general laboratory grade used as supplied unless otherwise specified. Microanalyses (C,H,N) were performed by Mrs A. Dams of this department. The ¹H and ¹³C NMR spectra were recorded on a Bruker WM360 spectrometer operating at 360 and 90 MHz respectively, electronic and circular dichroism spectra using Perkin-Elmer Lambda 5 and Jobin Yvon CNRS Dichrographe V spectrophotometers, respectively. The solid state CD measurements were performed on KBr discs containing the complexes as 1% dispersions in the oven-dried metal halide. The reported results are the average from 3–6 independent spectra for each complex. It is notable that little variation was observed on recording the spectra for the *N(S)* and *N(R)*-[Pd(*S*-meap)Cl₂] complexes; larger discrepancies occurred in the spectra of [Pd(*S*-ap)Cl₂].

Preparations

***N*-Benzyloxycarbonylasparagine.** To a vigorously stirred suspension of *S*-asparagine (10 g, 0.076 mol) in 1 M NaHCO₃ (150 ml) was added in portions over a period of 90 min, 11.4 ml (0.080 mol) of benzyloxycarbonyl chloride. After stirring for 2 h the mixture was extracted with Et₂O (1 × 150 ml), and the aqueous phase acidified to pH 1–2 with concentrated HCl precipitating a thick pasty solid. The white precipitate was collected, washed sparingly with cold water, air-dried and recrystallised from water, yield = 12 g (60%), mp = 159–161 °C (uncorrected). δ_H (d₆-dmsO) 12.66 (1 H, br, CO₂H), 7.47 (1 H, d, NH), 7.32 (5 H, s, C₆H₅), 6.92 (1 H, s, NH), 5.03 (2 H, s, CH₂), 4.34 (1 H, q, CH), 3.37 (1 H, br, NH) and 2.50 (2 H, m, CH₂).

***N*-Benzyloxycarbonylasparagine methyl ester.** Acetyl chloride (70 ml, 0.188 mol) was added dropwise to a stirred suspension of *N*-benzyloxycarbonylasparagine (50 g, 0.188 mol) in dry MeOH (500 ml) at –70 °C. After the addition the mixture was refrigerated at –15 °C overnight. The solvent was removed *in vacuo* at < 5 °C, and the residue treated with Et₂O until a solid had formed. The mixture was cooled overnight at –15 °C, filtered, and the white solid obtained washed with dry Et₂O, water and finally Et₂O to give the dry solid, yield = 52.5 g (99%), mp = 150–152 °C (uncorrected). δ_H (d₆-acetone) 7.36 (5 H, m, C₆H₅), 5.08 (2 H, s, CH₂), 4.54 (1 H, q, CH), 3.64 (3 H, s, CH₃) and 2.68–2.94 (5 H, m, NH and CH₂).

3-(Benzyloxycarbonylamino)-*S*-succinimide. To a stirred suspension of *N*-benzyloxycarbonylasparagine methyl ester (47 g, 0.168 mol) in water was added 325 ml of 0.5 M NaOH. After

stirring for 20 min the mixture was filtered and the filtrate acidified with 1 M HCl to give a thick precipitate. The solid was collected by filtration, washed with ice-cold water and air-dried. A single treatment with NaOH was not sufficient for complete conversion of the ester: unchanged material recovered during the initial filtration was treated once more with base to obtain the maximum yield of succinimide derivative. Recrystallisation was effected from ethyl acetate–light petroleum (bp 40–60 °C) yield = 27.5 g (66%) mp = 80 °C (uncorrected). δ_H (d₆-acetone) 10.14 (1 H, br, NH), 7.0–7.3 (5 H, m, C₆H₅), 6.68 (1 H, d, NH), 5.02 (2 H, s, CH₂), 4.34 (1 H, q, CH) and 2.66 (2 H, m, CH₂).

3*S*-(Methylamino)pyrrolidine dihydrochloride (*S*-meap·2HCl). A solution of 3-*S*-(benzyloxycarbonylamino)succinimide (10.9 g, 44 mmol) in dry THF (200 ml) was added dropwise to a rapidly stirred suspension of lithium aluminium hydride (7.5 g) in dry THF (500 ml). The mixture was set to reflux for 72 h, cooled, then hydrolysed at room temperature by the successive addition of water (7.5 ml), 15% aqueous NaOH (7.5 ml) and water (22.5 ml) to the rapidly stirred mixture. The mixture was stirred overnight and the aluminate cake filtered off and extracted with hot THF (2 × 200 ml). The filtrate and extracts were combined and the solvent removed *in vacuo* to give a dark oil. The oil was partitioned between 1 M HCl (300 ml) and Et₂O (300 ml) and the aqueous phase concentrated *in vacuo* to near dryness. Treatment of the residue with EtOH gave a crystalline solid which was filtered off, washed sparingly with cold EtOH, then triturated thoroughly with dry Et₂O to give a white solid, yield = 2.50 g (33%). *a*(589.3 nm, 20 °C, free amine, 2% in MeOH = –14.5°). δ_H (D₂O) 4.12 (1 H, m, CH), 3.87 (1 H, dd, CH), 3.55 (3 H, m, 3 CH), 2.81 (3 H, s, CH₃), 2.62 (1 H, m, CH) and 2.26 (1 H, m, CH).

[Ni(*S*-ap)]₂[ClO₄]₂. To a stirred solution of Ni(ClO₄)₂·6H₂O (1.15 g, 3.14 mmol) in MeOH (20 ml) was added a solution of 2 mol equivalents of *S*-ap (0.54 g) in MeOH (20 ml) giving an immediate yellow precipitate which was filtered off, washed with MeOH then Et₂O and air-dried. Yield = 0.55 g (41%) (Found: C, 22.6; H, 4.7; N, 12.9. Calc. for C₈H₂₀Cl₂N₄NiO₈: C, 22.35; H, 4.70; N, 13.03%). UV/VIS (methanol): λ_{max}/nm (ε/dm² mol^{–1}): 442 (750). CD (methanol): λ_{max}/nm (Δε/dm² mol^{–1}) 424 (+2.32).

[Cu(*S*-ap)]₂[ClO₄]₂·H₂O. As for the nickel(II) complex above, using Cu(ClO₄)₂·6H₂O. The initial purple solid product hydrated in air to give the blue monohydrate. Yield = 1.25 g (90%) (Found: C, 21.4; H, 4.5; N, 12.4. Calc. for C₈H₂₂CuCl₂N₄O₉: C, 21.22; H, 4.91; N, 12.38%). UV/VIS (water): λ_{max}/nm (ε/dm² mol^{–1}) 552 (1350). CD (water): λ_{max}/nm (Δε/dm² mol^{–1}) 587 (–0.63) and 504 (+0.81).

[Cu(*S*-ap)₂Cl]ClO₄. To a solution of [Cu(*S*-ap)]₂[ClO₄]₂·H₂O (0.5 g, 1.10 mmol) in MeOH (30 ml) was added 1.5 mol equivalents of LiCl·H₂O in MeOH (10 ml). After stirring for 10 min a blue precipitate had formed. The solid was filtered off, washed with minimum MeOH and air-dried. Yield = 0.22 g (54%) (Found: C, 26.1; H, 5.5; N, 15.1. Calc. for C₈H₂₀CuCl₂N₄O₄: C, 25.91; H, 5.45; N, 15.11%). UV/VIS (nitromethane): λ_{max}/nm (ε/dm² mol^{–1}): 636 (1900). CD (nitromethane): λ_{max}/nm (Δε/dm² mol^{–1}): 725 (+1.87), 576 (+0.55) and 470 (–0.10).

[Cu(*S*-ap)₂Br]ClO₄. As for the chloride complex above using 100 mg [Cu(*S*-ap)]₂[ClO₄]₂·H₂O and a 10% stoichiometric excess of LiBr in a total volume of 20 ml of MeOH. Diethyl ether was added to ensure complete precipitation of the ternary complex. This was collected at the pump, washed (Et₂O) and air-dried. Yield = 75 mg (83%) (Found: C, 23.2; H, 4.6; N, 13.3. Calc. for C₈H₂₀BrClCuN₄O₄: C, 23.4; H, 4.86; N, 13.50%). UV/VIS (nitromethane): λ_{max}/nm (ε/dm² mol^{–1}) 628 (1980). CD

(nitromethane): λ_{\max}/nm ($\Delta\epsilon/dm^2 mol^{-1}$) 754 (+2.36), 558 (+0.39) and 475 (-0.13).

[Cu(S-ap)₂][ClO₄]. As for the bromide, substituting LiI. Blue solid. Yield = 70 mg (70%) (Found: C, 20.9; H, 4.3; N, 12.2. Calc. for C₈H₂₀ClCuIN₄O₄: C, 20.79; H, 4.37; N, 12.12%). UV/VIS (nitromethane): λ_{\max}/nm ($\epsilon/dm^2 mol^{-1}$) 626 (2030). CD (nitromethane): λ_{\max}/nm ($\Delta\epsilon/dm^2 mol^{-1}$) 774 (+2.89), 615 (-1.51) and 472 (-0.67).

[Cu(S-ap)₂(SCN)ClO₄]. Prepared like the halides, but using NaSCN. Yield = 40 mg (46%) (Found: C, 27.6; H, 5.1; N, 17.7. Calc. for C₉H₂₀N₅ClSO₄Cu: C, 27.48; H, 5.13; N, 17.81%). UV/VIS (nitromethane): λ_{\max}/nm ($\epsilon/dm^2 mol^{-1}$): 624 (1670). CD (nitromethane): λ_{\max}/nm ($\Delta\epsilon/dm^2 mol^{-1}$) 839 (+0.94), 623 (-0.80) and 533(sh) (-0.34).

[Cu(S-ap)₂(NO₂)ClO₄]. As for thiocyanate, except using NaNO₂. Yield = 30 mg (40%) (Found: C, 24.9; H, 5.2; N, 18.0. Calc. for C₈H₂₀ClCuN₅O₆: C, 25.20; H, 5.30; N, 18.37%). UV/VIS (nitromethane): λ_{\max}/nm ($\epsilon/dm^2 mol^{-1}$) 611 (1390). CD (nitromethane): λ_{\max}/nm ($\Delta\epsilon/dm^2 mol^{-1}$) 720 (+0.71), 624 (-0.19), 554 (+0.32) and 473 (-0.09).

[Pd(S-ap)Cl₂]. To a stirred solution of K₂[PdCl₄] (0.92 g, 2.80 mmol) in water (10 ml) was added dropwise a solution of S-ap (2 mol equivalents) in water (10 ml). The mixture was heated to near boiling whilst maintaining the volume by periodic addition of water. The warm solution was filtered to remove a small deposit of elemental palladium and the filtrate cooled to ca. 10 °C. The cold solution was added dropwise to a stirred solution of K₂[PdCl₄] (0.92 g, 2.80 mmol) in water (10 ml) giving an immediate precipitate. The pink solid was filtered off, washed sparingly with cold water and air-dried. The dry solid was boiled in water (40 ml) containing several drops of concentrated HCl with occasional addition of further water to maintain the volume until a yellow solution was obtained (2–3 h). Upon cooling, golden yellow crystals were deposited. These were collected, washed sparingly with ice-cold water and air-dried. Yield = 0.60 g (40%). A second crop was obtained on concentrating the filtrate (Found: C, 18.3; H, 3.8; N, 10.7. Calc. for C₄H₁₀Cl₂N₂Pd: C, 18.23; H, 3.83; N, 10.64%). Yield = 0.22 g (15%). UV/VIS (0.2 M KCl), λ_{\max}/nm ($\epsilon/dm^2 mol^{-1}$): 372 (4210). CD (0.2 M KCl): λ_{\max}/nm ($\Delta\epsilon/dm^2 mol^{-1}$): 394 (-4.76), 356 (-1.06) and 327 (+1.42).

[Pd(S-ap)₂][PF₆]₂. To a solution of [Pd(S-ap)Cl₂] (0.22 g, 0.84 mmol) in water (10 ml) was added a solution containing S-ap (0.11 g, 1.28 mmol) in water (10 ml) and the whole heated near boiling with constant stirring for 1 h. After cooling, a solution of NH₄PF₆ (0.27 g, 1.68 mmol) in water (5 ml) was added. Concentration of the solution *in vacuo* led to the precipitation of the desired compound as colourless, feathery needles. These were filtered off, washed sparingly with water and air-dried. Yield = 275 mg (55%) (Found: C, 17.5; H, 3.6; N, 10.0. Calc. for C₈H₂₀PF₁₂N₄P₂Pd: C, 16.90; H, 3.55; N, 9.85%). UV/VIS (water): λ_{\max}/nm ($\epsilon/dm^2 mol^{-1}$) 289 (4280). CD (water): λ_{\max}/nm ($\Delta\epsilon/dm^2 mol^{-1}$) 321 (-2.87) and 278 (+6.84).

[Pt(S-ap)Cl₂]. To a stirred solution of K₂[PtCl₄] (2.35 g, 5.65 mmol) in water (100 ml) was added S-ap (0.54 g, 6.28 mmol) dissolved in water (20 ml) and the solution heated near boiling for 2 h before being cooled to room temperature overnight. The yellow solid that precipitated was filtered off, washed with water and air-dried. Yield = 1.10 g (55%) (Found: C, 13.6; H, 2.9; N, 7.9. Calc. for C₄H₁₀Cl₂N₂Pt: C, 13.64; H, 2.87; N, 7.96%). The complex was insoluble in common solvents and was converted into its diaqua analogue for UV/VIS and CD analysis by warming a suspension of the dichloro complex with 2 mol equivalents of silver(I) perchlorate in 2 M perchloric acid. UV/VIS (2

M HClO₄): λ_{\max}/nm ($\epsilon/dm^2 mol^{-1}$): 322 (530) and 259 (2090). CD (2 M HClO₄): λ_{\max}/nm ($\Delta\epsilon/dm^2 mol^{-1}$): 324 (+1.33) and 277 (-1.19).

[Pt(S-ap)(NH₃)₂Cl₂]. The complex [Pt(S-ap)Cl₂] (0.2 g, 0.57 mmol) was heated in aqueous ammonia (2 M) at 40–50 °C for 2 h. The solvent was removed and the resultant white solid washed sparingly in ethanol then diethyl ether and air-dried. Yield = 0.2 g (91%) (Found: C, 12.3; H, 4.1; N, 14.3. Calc. for C₄H₁₆Cl₂N₄Pt: C, 12.44; H, 4.18; N, 14.51%). UV/VIS (water): λ_{\max}/nm ($\epsilon/dm^2 mol^{-1}$) 284 (1040) and 227 (3780). CD (water): λ_{\max}/nm ($\Delta\epsilon/dm^2 mol^{-1}$) 284 (+0.16) and 241 (-0.45).

[Pt(S-ap)₂][PF₆][ClO₄]. To a stirred suspension of [Pt(S-ap)Cl₂] (0.3 g, 0.85 mmol) in water (15 ml) was added dropwise a solution of S-ap (0.11 g, 1.28 mmol) in water (5 ml). The mixture was heated near boiling with maintenance of volume for 2 h. After cooling to room temperature, solid NaClO₄·H₂O (0.24 g, 1.70 mmol) was added followed by solid ammonium hexafluorophosphate (0.28 g, 1.70 mmol). Concentration of the solution *in vacuo* gave the desired product as a white solid. Yield = 0.30 g (58%) (Found: C, 15.6; H, 3.2; N, 9.0. Calc. for C₈H₂₀ClF₆N₄O₄PPt: C, 15.70; H, 3.30; N, 9.16%). UV/VIS (water): λ_{\max}/nm ($\epsilon/dm^2 mol^{-1}$) 280 (560) and 222 (5860). CD (water): λ_{\max}/nm ($\Delta\epsilon/dm^2 mol^{-1}$): 278 (+2.64) and 237 (-3.05).

The complexes of S-meap were prepared in an analogous manner to those of S-ap, and only the relevant details of each complex are presented below.

[Ni(S-meap)₂][ClO₄]₂. As for S-ap. Yellow solid. Yield = 80% (Found: C, 26.2; H, 5.1; N, 12.4. Calc. for C₁₀H₂₄Cl₂N₄NiO₈: C, 26.22; H, 5.29; N, 12.24%). UV/VIS (water): λ_{\max}/nm ($\epsilon/dm^2 mol^{-1}$) 451 (940). CD (water): λ_{\max}/nm ($\Delta\epsilon/dm^2 mol^{-1}$) 441 (+5.68).

[Cu(S-meap)₂][ClO₄]₂. As for S-ap. Purple-blue solid. Yield = 90% (Found: C, 25.4; H, 5.1; N, 11.4. Calc. for C₁₀H₂₄CuCl₂N₄O₈: C, 25.95; H, 5.24; N, 12.11%). UV/VIS (water): λ_{\max}/nm ($\epsilon/dm^2 mol^{-1}$) 565 (1420). CD (water): λ_{\max}/nm ($\Delta\epsilon/dm^2 mol^{-1}$) 630 (-0.94) and 535 (+2.07).

[Pd(S-meap)Cl₂]. This complex was obtained in two distinct forms from aqueous solution: large orange blocks, the N_{Me}(R) isomer, and thin yellow plates, the N_{Me}(S) isomer. Overall combined yield = 60%. The two forms were readily separated by mechanical means, *i.e.* by inspection and hand separation or by flotation in slightly acidic water; the yellow plates are readily suspended on agitation and decanted off from the orange blocks. N_{Me}(R)-[Pd(S-meap)Cl₂] (Found: C, 21.7; H, 4.3; N, 10.2. Calc. for C₅H₁₂Cl₂N₂Pd: C, 21.64; H, 4.37; N, 10.10%). N_{Me}(S)-[Pd(S-meap)Cl₂] (Found: C, 21.7; H, 4.4; N, 10.1%): UV/VIS (0.2 M KCl) λ_{\max}/nm ($\epsilon/dm^2 mol^{-1}$) 376 (4280); CD (0.2 M KCl), λ_{\max}/nm ($\Delta\epsilon/dm^2 mol^{-1}$): 392 (-7.38) and 341 (+7.93). The spectra were the same irrespective of which solid isomer was used for the preparation of the solution for spectrophotometric analysis.

[Pt(S-meap)Cl₂]. Pale yellow solid. Yield = 50% (Found: C, 16.1; H, 3.4; N, 7.5. Calc. for C₅H₁₂Cl₂N₂Pt: C, 16.40; H, 3.31; N, 7.65%). UV/VIS (2 M HCl): λ_{\max}/nm ($\epsilon/dm^2 mol^{-1}$): 355(sh) (480), 303 (2320) and 277(sh) (1700). CD (2 M HCl), λ_{\max}/nm ($\Delta\epsilon/dm^2 mol^{-1}$) 379 (+0.44), 305 (-1.80) and 267 (+4.10).

X-Ray crystallography for [Pd(S-meap)Cl₂]

Crystallographic data for the orange N_{Me}(R) isomer of [Pd(S-meap)Cl₂] were collected on a FAST area detector diffractometer (rotating anode) by following previously described procedures.¹⁸ The cell dimensions were obtained by least-squares refinement of the diffractometer angles for 250 reflec-

tions ($3.32 \leq \theta \leq 29.71^\circ$). Intensities of 4313 reflections were collected within the same θ range ($-9 \leq h \leq 6$; $-13 \leq k \leq 14$; $-15 \leq l \leq 7$), and these yielded 2203 unique data with intensity > 0 ($R_{\text{int}} = 0.0230$). The data were corrected for absorption effects (DIFABS).¹⁹

Crystal data. $\text{C}_5\text{H}_{12}\text{Cl}_2\text{N}_2\text{Pd}$, $M = 277.49$, orthorhombic, space group $P2_12_12_1$ (no. 19), $a = 7.2131(4)$, $b = 10.595(2)$, $c = 11.664(4)$ Å, $U = 891.38$ Å³, $Z = 4$, $D_c = 2.068$ g cm⁻³, $\mu(\text{Mo-K}\alpha) = 26.12$ cm⁻¹, $\lambda(\text{Mo-K}\alpha) = 0.71069$ Å, $T = 150$ K, crystal size $0.20 \times 0.16 \times 0.12$ mm.

The structure was solved by direct methods (SHELXS 86)²⁰ and refined by full-matrix least squares on F^2 using all unique data (SHELXL 96).²¹ All non-hydrogen atoms were anisotropic, and the hydrogen atoms were included in calculated positions (riding model) with U_{iso} tied to the U_{eq} of the parent atoms. Final R (on F) and $wR2$ (on F^2) values were 0.0234 and 0.0548 respectively for all 2203 data and 92 parameters, $w = 1/[\sigma^2(F_o^2)]$. The Flack parameter²² [$-0.07(4)$] was close to 0 and this confirmed that the absolute structure has been determined correctly.

CCDC reference number 186/1298.

See <http://www.rsc.org/suppdata/dt/1999/599/> for crystallographic files in .cif format.

Acknowledgements

The authors are grateful to the EPSRC for funding and Professors R. D. Gillard and P. A. Williams for their considerable help during this study.

References

1 D. A. House, in *Comprehensive Co-ordination Chemistry*, eds. G.

- Wilkinson, R. D. Gillard and J. A. McCleverty, Pergamon, Oxford, 1987, vol. 2, p. 30.
- 2 M. Takamatsu, *Eur. Pat. Appl.*, 0 327 709 A2, 1988.
 - 3 V. Moreno, G. Cervantes, G. B. Onoa, F. Sampedro, P. Santaló, X. Solans and M. Font-Bardia, *Polyhedron*, 1997, **16**, 4297.
 - 4 F. P. Fanizzi, L. Maresca, G. Natile, M. Lanfranchi, A. M. Manotti-Lanfredi and A. Tiripicchio, *Inorg. Chem.*, 1988, **27**, 2422.
 - 5 M. Morita and S. Yoshikawa, *J. Chem. Soc., Chem. Commun.*, 1972, 578.
 - 6 H. Ito, J. Fujita and K. Saito, *Bull. Chem. Soc. Jpn.*, 1967, **40**, 2584.
 - 7 E. A. Sullivan, *Can. J. Chem.*, 1979, **57**, 67.
 - 8 B. Bosnich and E. A. Sullivan, *Inorg. Chem.*, 1975, **14**, 2768.
 - 9 Y. Nakayama, K. Matsumoto, S. Ooi and H. Kuroya, *Bull. Chem. Soc. Jpn.*, 1977, **50**, 2304.
 - 10 A. E. Sullivan, *Can. J. Chem.*, 1979, **57**, 62.
 - 11 O. P. Slyudkin, O. N. Adrianova, P. A. Chel'tsov and L. M. Volshtein, *Russ. J. Inorg. Chem. (Int. Ed.)*, 1973, **18**, 1398.
 - 12 T. J. Appleton and J. R. Hall, *Inorg. Chem.*, 1972, **11**, 117.
 - 13 K. Miyamura, M. Saburi, S. Tsuboyama, K. Tsuboyama and T. Sakurai, *J. Chem. Soc., Dalton Trans.*, 1988, 1543.
 - 14 K. Miyoshi, H. Tanaka, E. Kimura, S. Tsuboyama, S. Murata, H. Shimizu and K. Ishizu, *Inorg. Chim. Acta*, 1983, **78**, 23.
 - 15 K. Kamisawa, K. Matsumoto, S. Ooi, H. Kuroya, R. Saito and Y. Kidani, *Bull. Chem. Soc. Jpn.*, 1978, **51**, 2330.
 - 16 J. Iball, M. MacDougall and S. Scrimgeour, *Acta Crystallogr., Sect. B*, 1975, **31**, 1672.
 - 17 I. Bernal, *Inorg. Chim. Acta*, 1985, **96**, 99.
 - 18 J. A. Darr, S. R. Drake, M. B. Hursthouse and K. M. A. Malik, *Inorg. Chem.*, 1993, **32**, 5704.
 - 19 N. P. C. Walker and D. Stuart, *Acta Crystallogr., Sect. A*, 1983, **39**, 158.
 - 20 G. M. Sheldrick, *Acta Crystallogr., Sect. A*, 1990, **46**, 467.
 - 21 G. M. Sheldrick, SHELXL 96 Program for Crystal Structure Refinement, University of Göttingen, 1996.
 - 22 H. D. Flack, *Acta Crystallogr., Sect. A*, 1983, **39**, 876.

Paper 8/08959K